Addressing Range Anxiety in Electric Vehicles with Physics-Based Drivetrain Models and an Appropriate Charging Strategy

Romain Vanderbeeken[1](✉), Pierre Duysinx[1], and Yves Toussaint[2]

[1] University of Liege, Automotive Engineering, Liege, Belgium
romain.vanderbeeken@uliege.be
[2] Courant Alternatif Engineering, Liege, Belgium

AQ1

Abstract. The electric vehicles are often associated to the range anxiety phenomenon. In the paper, this is tackled by the elaboration of a set of physics-based drivetrain models aiming to accurately estimate the energy consumption of a medium class vehicle. After a convincing validation of the model with respect to the *VW ID*.3 WLTP ratings, some usual driving scenarios are investigated to identify eco-driving tips to help the EV driver optimize the use of its vehicle. The results indicate that a compromise should be found between the aerodynamic drag and the electrical Joule effects. Additionally, few charging loss computations are performed and indicate that it represents between 6 and 12% of the total charging energy.

Keywords: Electric Vehicles · Eco-Driving · Vehicle Simulation · Drivetrain Modelling · Charging strategy

1 Introduction

The electric vehicles are gaining in popularity for few years across the world. However, their range is generally lower than that of traditional vehicles. The fear of running out of energy during a journey is precisely designated as “range anxiety”, in such a way that an accurate understanding of the vehicle energy consumption is essential to correctly predict the remaining range. The paper addresses this phenomenon by elaborating an overall vehicle energy consumption model composed of physics-based power loss models of the main drivetrain components (for simplicity, the term *drivetrain* used here, indicates also battery and power electronics, not only the devices producing and transferring mechanical power). Therefore, the transmission, the motor, the inverter and the battery are individually investigated based on a large literature review to deeply understand and control the power loss sources.

To adequately face the range anxiety phenomenon, the precision of the vehicle model is of outmost importance. Its validation, for a given vehicle, over the WLTP driving cycle, is thus necessary before dealing with daily-life driving simulations. To this end, a MATLAB code allows to simulate the energy consumption associated to a given driving

A. Chiru and D. Covaciu (Eds.): CONAT 2024, PRAENG, pp. 1–12, 2025.
https://doi.org/10.1007/978-3-031-77627-4_3

scenario using a backward dynamic scheme. Starting from the road loads, the battery output power is determined by computing the output power at each previous drivetrain component. The main goal of the article being to provide eco-driving tips to an EV driver, the choice of the driving scenarios is important. For instance, in urban conditions, stops are very frequent. Hence, a case study aiming to identify the optimal speed profile between two stops is presented. A second case study concerning the crossing of a hill on a highway is discussed afterwards.

In addition to the vehicle energy consumption model, the paper also aims to provide energy loss information about some charging strategies. To adapt the discussion to real-life situations, the method relies on the driver needs, in terms of charging energy amounts, and on charging power levels corresponding to a medium class vehicle.

2 Physics-Based Eco-Driving Strategy

2.1 Equation of Motion

At a given speed, the vehicle motion is subject to road resistance forces, composed of the rolling resistance F_{rr}, the aerodynamic drag F_{aero} and the grading resistance F_{grad}. Road resistance must be overcome by the tractive force F_t. In acceleration, the acceleration force $m_e \frac{dV}{dt}$ adds to the resistance forces so that the equation of motion of the vehicle writes [1]

$$
\begin{aligned}
F_t &= F_{res} + m_e \frac{dV}{dt} \\
&= F_{rr} + F_{aero} + F_{grad} + m_e \frac{dV}{dt} \\
&= mgf_{rr} \cos\theta + \frac{1}{2}\rho S C_D V^2 + mg \sin\theta + m_e \frac{dV}{dt}.
\end{aligned} \tag{1}
$$

The rolling resistance stems from the hysteresis effect of rubber of the tire structure. As a result, the ground reaction presents an asymmetric pressure distribution which results in a resistive torque. For passenger car tires rolling on an asphalt road, a rolling resistance coefficient $f_{rr} = 0.01$ is often used [2].

The aerodynamic drag results from the air pressure distribution upon the vehicle and the skin friction effect along the vehicle body that produces a net resultant force towards the rear of the vehicle. At 20 °C, the air density, ρ, is 1.2 kg/m^3. A medium class vehicle is characterized by a frontal area S and a drag coefficient C_D such that $SC_D \approx 0.65$ [3].

The grading resistance is the component of the vehicle weight mg along the local backward direction when the road is inclined. The acceleration force is derived from Newton's second law of motion. The kinetic energy of the rotating parts in the drivetrain (wheels, gears, etc.) is taken into account by considering an equivalent vehicle mass m_e such that $m_e = \gamma m \approx 1.08m$ [3]. Note that these last two forces are negative in case of a downhill road and in deceleration. Given the slope and the deceleration, the tractive force may even become negative, resulting in an energy regeneration process with electrified vehicles (Eq. 1).

2.2 Physics-Based Drivetrain Models

In addition to the road resistance and acceleration forces, the powertrain components are multiple power loss sources. In order to precisely predict the energy consumption of a vehicle, it is appropriate to build a power loss model for each main component. Therefore, the transmission, the inverter, the motor and the battery are modelled based on torque T [Nm] − speed N [RPM] specifications of a medium class vehicle motor.

Transmission Stage. Considering a backward approach of the power flow, the transmission stage comes first once the road loads are computed. This stage comprises the gear pair and the differential. These components are subject to load-dependent and load-independent power loss [4]. On the one hand, power losses occur when the teeth are meshing (load-dependent losses). On the other hand, power losses permanently occur as soon as the gears rotate in the oil bath (load-independent losses) [5].

The power losses are computed for a medium class vehicle based on test bench experiment faced with literature results. The experiments are led with a 5-speed gearbox of a *Ford Escort* over a large operating region (between 750 and 6500 RPM and from 10 to 300 Nm) [6]. It includes both the gearbox and the differential power losses. Considering load-(in)dependent losses, the mechanical power loss writes

$$P_{loss,mech}(T, N) = a\left(TN\frac{2\pi}{60}\right)^b + c(N), \tag{2}$$

for which the load-independent term, $c(N)$, is determined by no-load tests.[1] The analysis of the measurements allows to determine a and b coefficients ($a = 0.00864, b = 1.1488$). From there, the mechanical power loss map in the full torque-speed plane is generated and represented in Fig. 1. It appears that the power loss evolve nearly linearly along the first bisecting line, up to 7 kW at maximum power output (150 kW). These results are consistent with results published in the literature [4, 5].

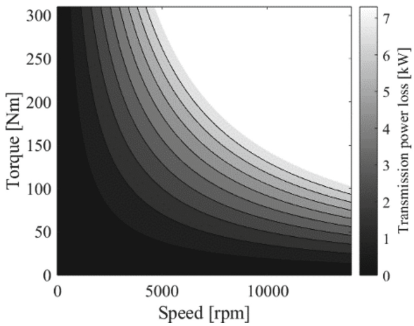

Fig. 1. Power loss map of the transmission stage (gear pair and differential)

Electric Motor. Modern passenger cars are equipped with permanent magnet (PM) motors thanks to their very high efficiencies and power to weight ratios [2]. These electric machines are composed of an iron rotor and copper stator windings fed with an

[1] The no-load tests are correlated to $c(N) = c_2N^2 + c_1N - c_0$ with. $c_2 = 1.46676 \cdot 10^{-8}\left[\frac{\text{W}}{\text{rpm}^2}\right]$, $c_1 = 0.8771 \cdot 10^{-4}\left[\frac{\text{W}}{\text{rpm}}\right]$ and $c_0 = 0.0266$[W].

electrical current. Both parts are subject to major power losses [3]. Indeed, hysteresis and eddy-current losses arise in the laminated rotor structure while the copper stator windings suffer from heat generation (Joule effects). Few windage losses also occur inside the motor [7].

In the literature, one can find a polynomial expression of the motor power losses [7]. By investigating the influence of the frequency (rotation speed) and the current (torque), a complete expression can be set:

$$P_{loss,mot}(T,N) = \sum\nolimits_{m,n=0}^{3} k_{mn}\left(\frac{T}{T_b}\right)^m\left(\frac{N}{N_b}\right)^n. \tag{3}$$

The parameters T_b and N_b respectively denote the maximum torque and the base speed, corresponding to the motor rotation speed at which maximum voltage is reached, that is at which the current starts to decrease to limit overheating [2]. The coefficients k_{mn} can be obtained either by lab tests or FEA [7, 8]. In the present work, the most important coefficients in Eq. 3 are identified based on theoretical results [3]. Dealing with the Volkswagen ID.3 motor, their values are then determined to fit with a similar work, for which the motor has the same technology and have similar ratings but some negative coefficients [8]. Table 1. Summarizes k_{mn} values, accompanied by the main source (Fe, Cu, Windage). The motor is characterized by $T_b = 310$ Nm and $N_B = 4620$ RPM [9].

From Eq. 3, the motor power loss map can be generated similarly as for the transmission stage and is reported in Fig. 2. It can be seen that moderate power loss levels, comparative to the transmission, are obtained over the whole map (max. 6 kW at maximum torque, close to base speed). Below 200 Nm, the power loss is particularly low whatever the rotation speed (less than 3 kW).

Table 1. Coefficients values of the motor power loss polynomial expression (Eq. 3)

k_{mn}	N^0	N^1	N^2	N^3
T^0		2344 (Fe)		77 (Windage)
T^1			346 (Fe)	
T^2	1216 (Cu)	2040 (Fe)		
T^3	2176 (Cu)			

Inverter. Between the motor and the battery, the drivetrain of an electric vehicle hosts the inverter whose role is to feed the motor with alternative current from the high voltage battery, or when appropriate, to charge the battery if the motor acts as a generator in energy regeneration periods. Since the inverter is a power electronics device, its power loss map is influenced by load-dependent and stand-by losses. The former mainly result from Joule effects while the latter result from constant power consumption to ensure its proper functioning. Based on literature results and lab experiment for an IGBT inverter (in the BMW i3) [10, 11], the power loss expression writes

$$P_{loss,inv}(T) = 300 + 1600\left(\frac{T}{T_b}\right)^2. \tag{4}$$

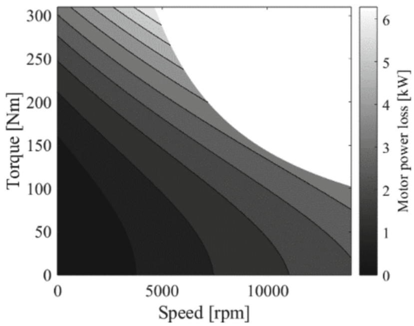

Fig. 2. Power loss map of the electric motor (permanent magnet technology)

Therefore, the power loss is independent of the rotation speed, quadratic in terms of the torque and varies between 300 and 1900 W. Compared to the previous components, these loss levels are a bit smaller at low speeds and much smaller at higher regimes.

Battery. Inside an electric vehicle, the battery pack is composed of numerous cells, assembled into modules themselves connected in series and in parallel. By electrochemical reactions in an electrolyte between two electrodes, the battery produces an electrical current that feeds the electric motor. The power loss model of the battery is quite different from the previous models due to the various factors influencing the battery losses. Indeed, although it is well known that the power is proportional to the product between the voltage and the current, the estimation of the power losses also strongly depends on the state of charge (SOC, opposite to the Depth of Discharge) of the battery since the voltage varies from a maximum to a minimal during a full discharge (from 4.2 V and 2.5 V for an Nickel-Manganese-Cobalt battery).

Additionally, the cells are the location of many irreversible processes [12]. One of the main processes deals with the polarization process, which results in a charge transfer resistance. This polarization effect comes from the voltage difference between the voltage corresponding to a given current at a given SOC and the open-circuit voltage (OCV) at the same SOC. The phenomenon is illustrated in Fig. 3., whose data come from a cell of the *VW ID.3* battery (here 1C = 78 A) [9]. The power loss, expressed in Eq. 5, is thus deduced based on the state of charge (i.e., voltage difference), the cell current (half of the battery current since the battery is composed of two rows mounted in parallel) and the total number of cells ($n_{cells} = 216$ for the *VW ID.3* battery):

$$P_{loss,bat} = n_{cells} \cdot \Delta V(SOC, I_{cell}) \cdot I_{cell}. \quad (5)$$

2.3 Applications

As mentioned in the introduction, the loss models of the drivetrain components are an added value to predict the energy consumption of a vehicle following a certain speed profile $V(t)$ [kph]. Over its total duration, the energy consumption is obtained by integrating the total instantaneous power:

$$E_{net} = \int P dt. \quad (6)$$

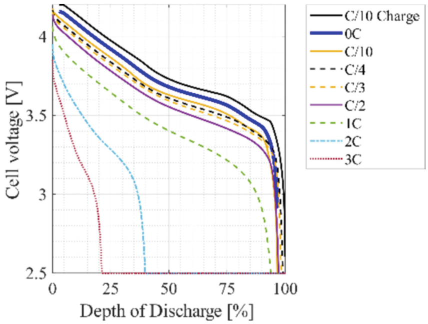

Fig. 3. Iso-current discharge voltage curves of a *VW ID.3* battery cell [9]

The total power is the sum of the power generated by the driving resistances, the acceleration power and the power losses in each powertrain component:

$$P(t) = P_{res}(t) + m_e \frac{dV}{dt} \cdot \frac{V(t)}{3.6} + P_{loss,mech}(T_{me}, N, t) + P_{loss,mot}(T_{mo}, N, t) + P_{loss,inv}(T_i, t) + P_{loss,bat}(SOC, I_{cell}, t) \tag{7}$$

Then, since the speed is known at any time, it is possible to derive the individual power losses following the backward approach. On the one hand, the vehicle speed can be linked to the motor rotation speed thanks to the reduction ratio i and the calculus radius R_c (assumed equal to the effective rolling radius, itself assumed equal to the dynamic radius). On the other hand, the instantaneous torque can be linked to the required output power at the drivetrain component k thanks to the rotation speed:

$$\begin{cases} N(t) = \frac{V(t)}{3.6} \cdot \frac{i}{R_c} \cdot \frac{60}{2\pi} [\text{RPM}]; \\ T_k(t) = \frac{P_{out,k}(t)}{N(t)} \cdot \frac{60}{2\pi} [\text{Nm}]. \end{cases} \tag{8}$$

The numerical applications are performed with a test car having the mass and the aerodynamic properties of the *VW ID.3* (Table 2). Concerning the battery, the cell current is determined based on an initial given SOC (60%) and by considering each current (Fig. 3) multiplied by the corresponding cell voltage and the total number of cells. Then, the selected current corresponds to the closest value from the required power output. To increase the precision, an iterative process is implemented by performing a linear interpolation of the voltage around the selected current. The relative error must be below 0.1% in terms of power output to end the iterative process.

Before applying the case studies, the complete model can be used to predict the energy consumption of the vehicle according to the WLTP driving cycle. It results in a vehicle consumption of 131.35 Wh/km. Compared to 135 Wh/km, it corresponds to a relative error of −2.7% [13].[2] Moreover, it can be shown that the rolling resistance

[2] The official energy consumption for the WLTP accounts for charging losses too, and increases the consumption to 153 Wh/km [13].

Table 2. Vehicle characteristics [3, 9]

$\boldsymbol{m} = \mathbf{1890}\,\text{kg}$	$\boldsymbol{S} = \mathbf{2.47}\,\text{m}^2$	$\boldsymbol{i} = \mathbf{11.53}$
$\boldsymbol{f_{rr}} = \mathbf{0.01}$	$\boldsymbol{C_D} = \mathbf{0.263}$	$\boldsymbol{R_c} = \mathbf{0.35}\,\text{m}$

and the aerodynamic drag together only count for 74% of the computed value, meaning that the remaining 26% come from power losses in the drivetrain. Hence, it reinforces the confidence in the fact that the consideration of these power losses is of outmost importance. Moreover, this consideration seems to be very accurate. To be complete, the total energy loss in the drivetrain is distributed equally between the transmission, the inverter and the battery (5% each), with the 11% remaining for the motor only.

Thanks to this validation, the case studies listed in the introduction can be investigated with confidence. The first case study deals with trapezoidal speed profiles while the second one deals with the crossing of a hill.

Case Study 1: Trapezoid Speed Profiles. For a given input dataset, this case study aims to identify the acceleration, constant speed, deceleration profile for which the energy consumption is minimized. For conservative reasons, the initial and final speeds must be identical, as well as the mean speed for each cycle. Urban conditions are chosen such that the mean speed is 30 kph, with a maximum allowable speed of 50 kph. The cycle is 60-s long and considers 0.5 km travel on a flat road. Concretely, this speed profile corresponds for instance to a route between two stops, which happens with a highly frequency in an urban environment.

For these input specifications, either the acceleration can be strong so that the constant speed can be low (i.e., an *aggressive* driving style), or the acceleration can be very smooth but the constant speed must be much higher to validate the mean speed condition (i.e., a *progressive* driving style). Following the procedure described in the beginning of the subsection, the energy consumption associated to 20 different speed profiles is reported in Fig. 4. Each profile refers to a constant speed running from 31 to 50 kph (from left to right). The abscissa informs about the corresponding acceleration; the most aggressive profile leads to an acceleration of 4.5 m/s^2, teasing the maximum capacity of the vehicle. The acceleration rapidly falls to less than 1 m/s^2. Since the energy consumption results from a complex model, the eco-driving tip results itself from a compromise between the power consumption of each contribution.

The Fig. 4 indicates that the speed profile minimizing the energy consumption for such conditions is characterized by an acceleration of 1.35 m/s^2 and a plateau speed of 34 kph. The energy consumption is 49.17 Wh. At the opposite, it can be seen that the most aggressive driving style, in addition to raising questions about road safety, is the less energy-saving (57 Wh, +15.9%) and is strongly penalized by Joule effects occurring in the electrical components, mainly the battery and the motor since the acceleration is correlated to the torque, itself linked to the current.

On the right in Fig. 4., the energy consumption increases constantly and reaches 53.36 Wh (+8.5%) with the lowest acceleration (0.58 m/s^2, 50 kph as constant speed). Even if Joule effects are minimized for such a profile, the aerodynamic drag becomes the most influencing factor, even for the present urban conditions, as soon as the acceleration is well lowered.

As a final discussion for this case study, the consideration of another vehicle may slightly change the eco-driving tip that is established here for the *VW ID.3*. Indeed, a heavier vehicle would be associated to an optimal speed profile with a lower acceleration and a higher plateau speed, since the acceleration, strongly influencing the power losses in the electrical components, is more energy-consuming as the mass increases. Conversely, the less a car is aerodynamic, the lower the constant speed value associated to the most energy-saving profile will be.

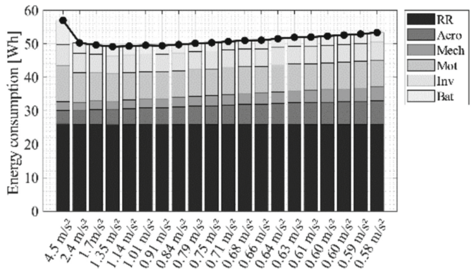

Fig. 4. Energy consumption of the driving profiles studied for the trapezoidal speed profiles (urban conditions, 0.5 km)

Case Study 2: **Hill Crossing**. This second case study deals with the crossing of a 5% inclined hill for which extra-urban conditions are assigned. Hence, the mean speed is fixed to 105 kph and the speed profiles have a “V-shape” time evolution: the speed difference between initial speed and the speed at the summit ranges from 0 (cruise control case) to 30 kph. For the latter, the initial speed is thus 120 kph while the speed linearly decreases to 90 kph when reaching the summit. The downhill part is characterized by the exact transpose of the uphill part. The total distance is 3.5 km, travelled in two minutes.

In a similar manner as the previous case study, the energy consumption for each speed profile investigated is reported in Fig. 5. The abscissa refers to the speed difference between the initial speed and the speed at the summit. The results indicate that this speed difference should be maximized to minimize the energy consumption. Indeed, for the 120-90-120 kph speed profile, the energy consumption is 565.8 Wh while the cruise control profile leads to 583 Wh (+3.04%). This increase comes from the battery power loss. Since absolutely no slowdown of the speed is allowed, the power consumption in that component has the highest mean value among the profiles. It is interesting to see that only a speed difference of 2 kph decreases a bit the consumption (570.5 Wh).

Although the eco-driving tip associated to this case study results in a lower variation of the energy consumption between the studied profiles, it is not less interesting since it is associated to a much higher magnitude. Moreover, the input specifications also play a role in the quite constant results since the speed difference may be increased if a speed greater than 120 kph is allowed. It can be shown that when considering a 130-100-130 kph profile, the energy consumption still decreases. Finally, since the aerodynamic drag represents a bit more than the half of the total consumption, it is clear that a less aerodynamic vehicle could present an increasing consumption with an increasing speed difference, since the aerodynamic drag is linked to the velocity squared.

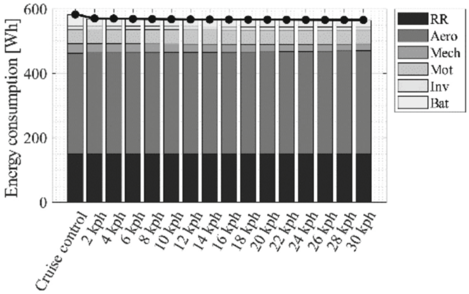

Fig. 5. Energy consumption of the driving profiles studied for the hill crossing speed profiles (extra-urban conditions, 3.5 km)

3 Charging Strategy

In line with the discussion about minimizing the energy consumption when the vehicle is riding, it is also interesting to quantify the energy loss during the charging of the EV. In the following, a model of the battery power losses in charging is computed. Moreover, additional losses arise in the power electronics and along the distribution network.

3.1 Battery Model

The charging battery model is very similar to the corresponding discharging model (Fig. 3. Iso-current discharge voltage curves of a *VW ID.3* battery cell [9]). The iso-current voltage curves still correspond to the *VW ID.3* and are represented in Fig. 6 [9]. Compared to Fig. 3, there are 5 charging currents from which the power losses can be computed exactly like those in discharging (Eq. 5).

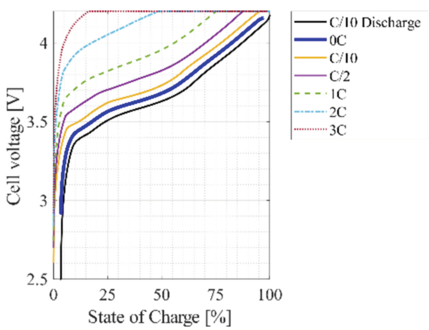

Fig. 6. Iso-current charge voltage curves of a VW ID.3 battery cell [9]

3.2 Others

Even if it can be expected that the battery power losses represent a major part of the total charging losses, a more complete model may help to increase the precision. In the literature, some charging power losses experiments are led. In the next applications, a 5% power loss occurring in the power electronics is considered [14]. However, it can be shown that the power loss from the distribution network is almost negligible so that the battery and the power electronics will be the only contributors.

3.3 Applications

The charging loss model is applied, firstly, to investigate the effect of the SOC interval and, secondly, to estimate the proportion of energy lost during a full fast recharge.

Influence of the State of Charge. Based on the iso-current voltage curves in Fig. 6, it can be observed that the battery power loss may vary depending on the SOC interval along which the charging process is performed. Indeed, for a given current, the voltage difference with the open-circuit voltage (OCV) curve is slightly variable. For the highest currents, once the cell voltage has reached 4.2V, the current is necessarily decreased.

Pursuing with the *VW ID.3* battery data, it is chosen to charge an amount of energy corresponding to half of the battery capacity that is 29 kWh [9]. From the WLTP results, it corresponds to about a 200 km range. Four SOC windows and the lowest three cell currents are compared in terms of power loss. Concretely, only the low (<10%) and high (>90%) extreme SOC are avoided since it is well known that irreversible capacity losses arise when these SOC values are attained [12]. The battery charging currents and powers correspond to 15.6 A, 78 A and 156 A and respectively 5.9 kW, 30.2 kW and 62.5 kW at 10% SOC.

The energy loss is reported in Fig. 7 for each scenario. For the lowest current, no influence on the SOC is found since the corresponding voltage curves always follows closely the OCV curve (Fig. 6). The amount of energy loss is lower than 0.5 kWh, i.e. less than 1.7% of the paid energy. For both higher currents, it can be seen that low SOC should be avoided since it leads to the higher energy losses compared to high SOC: compared to the 40–90% SOC interval, the losses with the 10–60% SOC window increase by up to 11% at 78 A (Fig. 7, C/2 is the cell current) and 13% at 156 A (1C). At the same time, for the same net recharged energy, the losses double between the 78 and 156 A currents, suggesting a clear influence of the polarization effect, from about 1 to 2 kWh [12]. With the power electronics losses, the energy loss reaches between 8 and 11% of the paid energy.

Fast Charging. Over a large fast charge, the battery allows a maximum charging power of 80 kW, from 10 to 80% SOC [13]. This second example proposes to compute the energy loss associated to this scenario, with a 1C cell current since its voltage curve is associated to a charging power between 58 and 66 kW. To charge the required 40.6 kWh, 3.01 kWh are lost in the battery (i.e., 6.9% of the total charging energy). Adding the loss in the power electronics unit, the total energy loss becomes 12.5%.

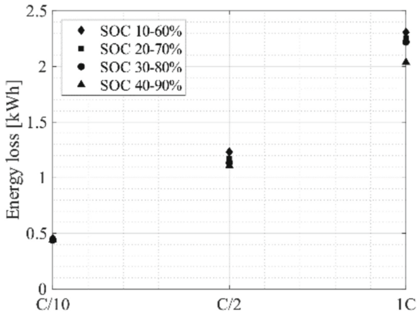

Fig. 7. Charging energy loss depending on the cell current and the SOC (1C = 78 A)

4 Conclusion

The control of the energy consumption of an electric vehicle is strongly important since its driving range is generally quite low. With the help of a plurality of power loss powertrain elements models developed from lab experiment and results from the literature, the energy consumption of a vehicle whose main characteristics are those of the *Volkswagen ID.3* is accurately estimated. Indeed, the results of the model applied to the WLTP driving cycle showed a relative error of less than 3% compared to published results, and the drivetrain (battery and electronics included) power losses contribute to 26% of the total energy consumption over this cycle. Thus, it validates the need of an accurate drivetrain model.

In a second step, two case studies inspired from daily-life situations are modeled to establish eco-driving tips for EV drivers. The investigation of a route between two stops in urban conditions taught that aerodynamic effects dominate if Joule effects in the electric device are low enough. Between different speed profiles, the energy consumption may increase by nearly 16%. The second case study dealt a route crossing a hill on a motorway. Imposing a 105 kph mean speed, the speed profiles compares the cruise control case with high speed difference between the foot and the summit of the hill. For the vehicle of interest, the larger the speed difference, the lower the energy consumption even if it remains in a 3% variation interval.

The computation of charging losses is finally studied. Depending on the state of charge and of the charging current, the loss levels are comprised between 6 and 12 kW.

References

1. Gillespie, T.D.: Fundamentals of Vehicle Dynamics. SAE International (2021)
2. Ebrahimi, K., Yimin, G., Longo, S., Ehsani, M.: Modern Electric, Hybrid Electric, and Fuel Cell Vehicles. CRC Press (2018). https://doi.org/10.1201/9780429504884
3. Robert Bosch GmbH: Automotive Handbook. Wiley (2022)
4. Petry-Johnson, T.T., Kahraman, A., Anderson, N.E., Chase, D.R.: Experimental investigation of spur gear efficiency. In: Volume 7: 10th International Power Transmission and Gearing Conference, pp. 747–758. ASMEDC, Las Vegas, Nevada, USA (2007). https://doi.org/10.1115/DETC2007-35045

5. Leprince, G.: Pertes mécaniques par frottement et lubrification dans une boîte de vitesses (2011)
6. Toussaint, Y.: Ford transaxle losses
7. Mahmoudi, A., Soong, W.L., Pellegrino, G., Armando, E.: Loss function modeling of efficiency maps of electrical machines. IEEE Trans. Ind. Applicat. **53**, 4221–4231 (2017). https://doi.org/10.1109/TIA.2017.2695443
8. Laitinen, H.: Improving Electric Vehicle Energy Efficiency with Two-Speed Gearbox (2017)
9. Wassiliadis, N., et al.: Quantifying the state of the art of electric powertrains in battery electric vehicles: range, efficiency, and lifetime from component to system level of the Volkswagen ID.3. eTransportation **12**, 100167 (2022). https://doi.org/10.1016/j.etran.2022.100167
10. Gurpinar, E., Ozpineci, B.: Loss analysis and mapping of a SiC MOSFET based segmented two-level three-phase inverter for EV traction systems. In: 2018 IEEE Transportation Electrification Conference and Expo (ITEC). pp. 1046–1053. IEEE, Long Beach, CA, USA (2018). https://doi.org/10.1109/ITEC.2018.8450188
11. U.S. Department of Energy, Office of Energy Efficiency & Renewable Energy: FY 2016 Annual Progress Report for Electric Drive Technologies Program (2017)
12. Ma, S., et al.: Temperature effect and thermal impact in lithium-ion batteries: a review. Prog. Nat. Sci. Mater. Int. **28**, 653–666 (2018). https://doi.org/10.1016/j.pnsc.2018.11.002
13. Volkswagen ID.3 Pro. https://ev-database.org/car/1831/Volkswagen-ID3-Pro. Accessed 31 May 2024
14. Apostolaki-Iosifidou, E., Codani, P., Kempton, W.: Measurement of power loss during electric vehicle charging and discharging. Energy **127**, 730–742 (2017). https://doi.org/10.1016/j.energy.2017.03.015